TESTING OF AN ELECTRIC MOTOR AS A STRUCTURE-BORNE SOUND SOURCE

A T Moorhouse University of Salford
R D Cookson University of Liverpool
G Seiffert University of Liverpool

1 INTRODUCTION

The background to this study is the increasing incentive for manufacturers of all types of machinery and equipment to cut the cost of prototype testing and speed up the process. 'Virtual Acoustic Prototypes' (VAPs) is an attractive prospect to meet these demands. A VAP is a 'virtual machine' which produces a realistic impression of the sound from the real assembled machine it represents. To be useful in prototyping the virtual machine must be 'assembled' from interchangeable components, each of which is represented by a data base of vibro-acoustic properties. Such virtual components can be combined rapidly in the computer to give an impression of what the machine will sound like before a physical prototype is built, thereby cutting cost and adding convenience.

The simplest way to breakdown a machine into components is to separate the 'active' components (motors, fans, pumps, compressors etc) which initially generate the noise from the remaining, purely passive parts of the machine. Therefore, at least two data sets are required for a VAP, one for active components which represents the excitation, and another for passive components which represents the 'colouration' effects of frequency-dependent transmission and radiation.

The work reported in this paper is part of a study to assemble a data set, suitable for use in VAPs, to describe one of the most common of active components, an electric motor. We focus here particularly on characterisation of the motor as a structure-borne sound source. It is necessary also to include airborne excitation from the motor in the VAP, but this is reported elsewhere.

When an active component like an electric motor excites a passive machine frame, the radiated sound pressure can be expressed at each frequency as the product of a vector of applied forces and a matrix of transfer functions:

$$\mathbf{p} = \mathbf{T}\mathbf{f} \tag{1}$$

where $\mathbf{p}$ is the external sound pressure, $\mathbf{f}$ is a vector of forces by the motor at the contact points and $\mathbf{T}$ a matrix of transfer functions, each element of which t_{ij} quantifies the sound pressure output at external position *i* per unit force input at excitation position *j*. The applied forces, $\mathbf{f}$, can in turn be written in terms of the free velocity of the source and the mobilities of source and receiver as:

$$\mathbf{f} = \left[\mathbf{Y}_S + \mathbf{Y}_R\right]^{-1}\mathbf{v}_{Sf} \tag{2}$$

where $\mathbf{v}_{Sf}$ is the vector of free velocity of the source, $\mathbf{Y}_S, \mathbf{Y}_R$ are the mobility matrices of the source and receiver. By substituting equation 2 into equation 1 the external sound pressure is given in terms of independent properties of the active and passive components:

$$\mathbf{p} = \mathbf{T}\left[\mathbf{Y}_S + \mathbf{Y}_R\right]^{-1}\mathbf{v}_{Sf}\,. \tag{3}$$

The required properties of the active component, in this case the motor, are seen to be the free velocity and the mobility matrix. The measurement of free velocity is now outlined in a standard [1]. It involves suspending the machine on a soft foundation and running it normally. The free velocity of an electric motor can be measured according to this methodology, but not whilst loaded. Since loading can be expected to alter the generation mechanisms, for example magnetic forces are expected to vary with load, then testing without load does not necessarily provide the data needed for the VAP. Therefore, an alternative is required.

An alternative to the free velocity is to characterise the activity of the motor by the blocked forces, i.e. the contact forces with the source connected to an infinitely rigid base with the motor operating normally. The contact forces are then given as:

$$\mathbf{f} = \left[\mathbf{Y}_S + \mathbf{Y}_R\right]^{-1}\mathbf{Y}_S\mathbf{f}_{Sb} \,. \tag{4}$$

where $\mathbf{f}_{Sb}$ is the vector of blocked forces. This formulation offers the potential advantage that the motor can be loaded, so that the VAP realistically represents the machine in operation, but there are no existing standard methods of measurement. The aim of this paper is therefore to investigate methods of obtaining the blocked force, and the specific objective is to measure and validate blocked forces for a 3kW electric motor.

A test rig has been developed where the motor is mounted to a rigid block (figure 1). The motor is loaded in two ways, firstly with a belt drive which provides a static lateral load, and secondly with a silent ‘eddy current brake’ which provides a resistive torque. Previous tests (to be reported elsewhere) had shown that loading does affect both airborne and structure-borne generation, which confirmed the need for testing under load. Since the emphasis of this paper is validation of the method of obtaining blocked forces, all the tests were conducted with the motor unloaded. However, the rig as shown can be used for testing under load once a measurement methodology has been established.

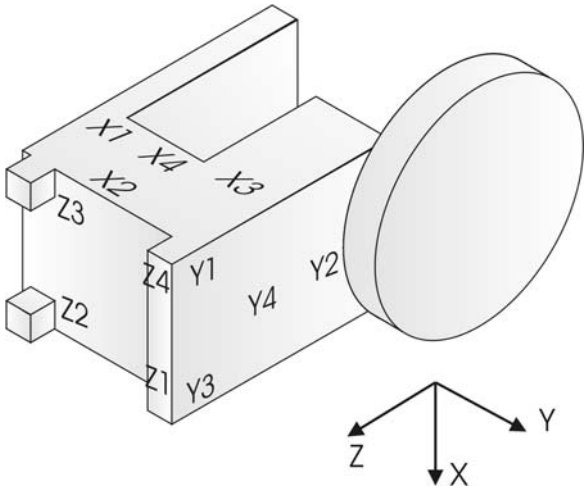

Figure 1: Test block. Left: with motor, showing pulley and eddy current brake. Right: as modeled for calculation of accelerance matrix

The test block was designed to be as mass-like as possible, with a mass of ten times that of the motor. It was confirmed by mobility measurements that the blocked condition was achieved across the frequency range of interest, ie 50-2000Hz (see figure 2), except in a narrow frequency range at the anti-resonance frequencies of the motor where the difference in mobility was less than 10dB. The block was made as compact as possible, particularly local to the connections with the motor. It was also made slender so as to have minimal effect on airborne sound emission, and measurement showed that its presence negligibly affected the sound power. This block arrangement is attractive

because when suspended away from walls and floor the free field airborne sound power and the blocked forces can potentially be measured simultaneously.

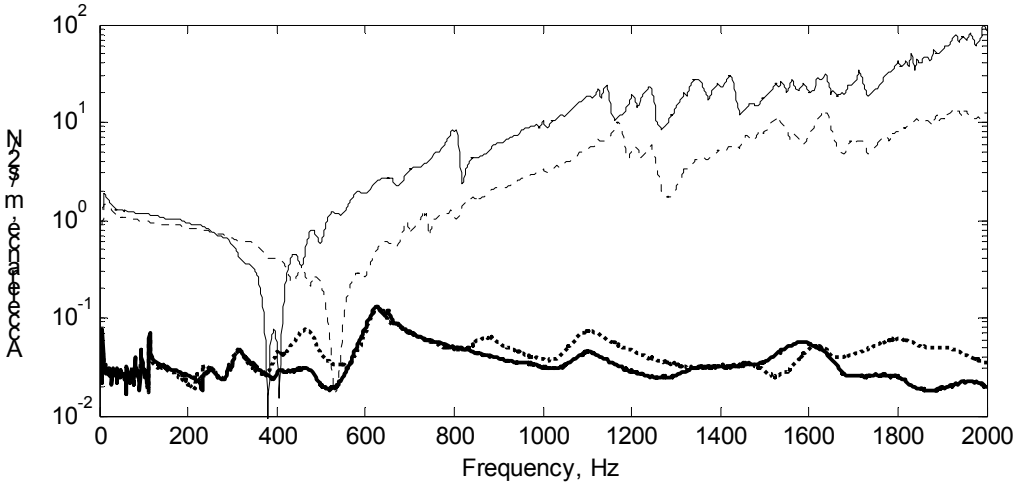

Figure 2: Point accelerance magnitude of mounting block and motor showing anti-resonance frequency f_L at around 400-500Hz

Two methods of blocked force measurement were tested. The first uses force transducers inserted between the block and the feet, and second makes use of an inverse method in which forces are back-calculated from the acceleration of the block.

2 MEASUREMENT USING FORCE TRANSDUCERS

The first measurement of blocked force was carried out by inserting four force transducers between motor and block. Single direction transducers were used at each of the four feet measuring force in the axial (y) direction. It would potentially have been possible to use tri-axial transducers and to measure simultaneously the x, y, and z direction forces at the four feet, a total of twelve forces, but none were available. The accelerometer mountings were carefully designed so as to remove as little material from the block as possible since it was anticipated that local stiffness would start to become significant at the high end of the frequency range. Also, thin, flat transducers were chosen to minimise 'rocking'.

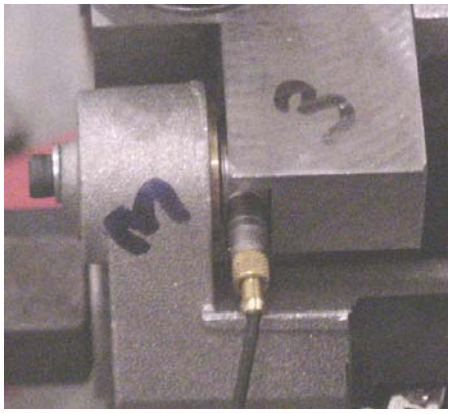

Figure 3: Motor lug showing force transducer for direct force measurement

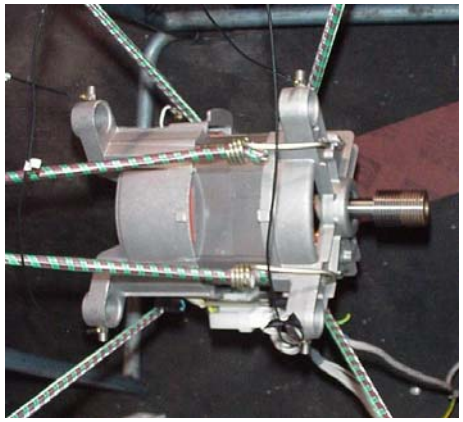

Figure 4: Motor resiliently mounted for measurement of free velocity

Two motors were tested at four speeds, plus one of them was run at an additional lower speed. The two motors were nominally identical structurally, but differed in their electrical drive. Motor A was an AC drive, and motor A2 a DC drive, both of which ran off 240V , 50Hz mains supply, and were fitted with brushes.

2.1 Validation

The question of how independently to validate the measured blocked forces needs careful consideration. If the system is linear, then the free velocity and blocked forces are related as follows:

$$\mathbf{f}_{\mathbf{Sb}} = \mathbf{Y}_{\mathbf{S}}^{-1}\mathbf{v}_{\mathbf{Sf}} . \tag{5}$$

Using equation 5, the blocked forces can be calculated from the free velocity if the mobility matrix is known. This then provides and independent estimate of the blocked forces which can be compared with measured values. However, since equation 5 requires a matrix inversion, which are notorious for numerical errors, a more reliable validation is to use it in reverse, in other words to compare the measured free velocity with that calculated from the blocked force using:

$$\mathbf{v}_{\mathbf{Sf}} = \mathbf{Y}_{\mathbf{S}}\mathbf{f}_{\mathbf{Sb}} . \tag{6}$$

The mobility matrix for motor A was already available, having been obtained by a novel combination of measurement and calculation as described in [2]. This matrix had been validated by several tests. The mobility matrix for motor A2 was assumed identical. In reality, this is probably a reasonable assumption at low frequency when the mobility is mass controlled, although some differences in detail would be expected at higher frequency when the local stiffness of the mounts becomes important.

The free velocity of the motor was measured by suspending the motor resiliently in free space using elasticated cords as shown in figure 4. Accelerometers were mounted on the attachment lugs to determine the measured free acceleration $\mathbf{a}_{\mathbf{Sf}}$ of the motor. The free velocity $\mathbf{v}_{\mathbf{Sf}}$ was determined using the relationship,

$$\mathbf{v}_{\mathbf{Sf}} = \mathbf{a}_{\mathbf{Sf}} / j\omega \tag{7}$$

Comparison can be made on a foot by foot basis, but a more reliable measure of the overall agreement is to use the spatial mean free velocity, i.e. the energy average of the velocity over the four feet. Therefore at each frequency the ‘overall’ free velocity is compared, defined by:

$$\bar{v}_{Sf} = \sqrt{\mathbf{v}_{\mathbf{Sf}}^{*\mathbf{T}}\mathbf{v}_{\mathbf{Sf}}} = \sqrt{v_{Sf1}^{\ 2} + v_{Sf2}^{\ 2} + v_{Sf3}^{\ 2} + v_{Sf4}^{\ 2}} \tag{8}$$

2.2 Discussion of results

Results are shown in narrow and third octave frequency bands in figure 5. The solid line is the directly measured overall free velocity and is taken as the ‘true’ reference. The estimate based on blocked force is given in dotted lines. Up to about 800Hz the general signature is in good agreement. Third octave values are mostly within 5dB up to about 500Hz, although there are occasionally bands with errors of more than 10dB, both under and over estimates. Above about 1kHz there is a systematic underestimation in the blocked force results. These results are for motor A, and are somewhat better than for motor A2.

It is believed that this is the first time such a comparison between free velocity and blocked force has been made. However, it is useful to look at the results of comparable types of calculations from

the literature. In reference [2], the measured and calculated contact velocity were compared when a source was connected to a receiver. In [3] the power was compared. In these cases and many others the predicted quantity shows broad agreement with the measured one, but with errors at some frequencies that can exceed 10dB. The current results look similar, perhaps better than typical results below 1000Hz. Above about 1000Hz there seems to be a systematic error.

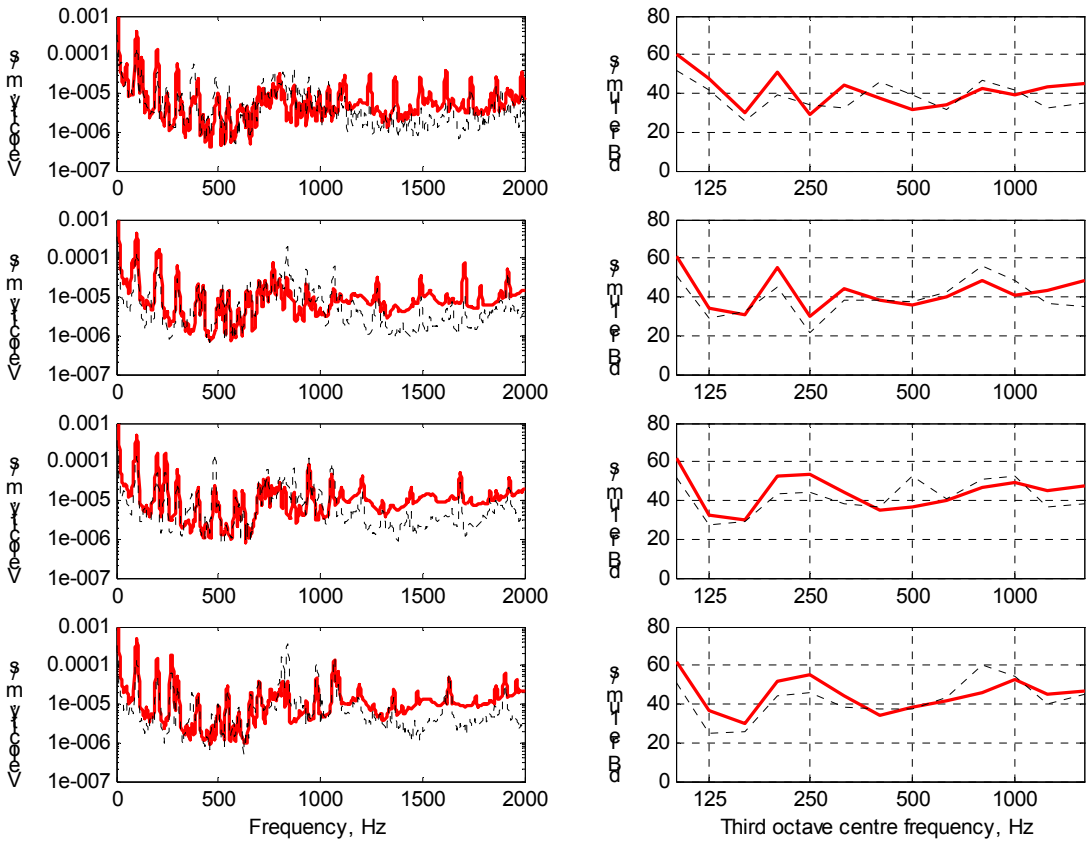

Figure 5: Motor A results for force transducer measurements: ¯ measured free velocity, --- calculated at running speeds of, from top to bottom 7436, 12688, 14352 and 16224 rpm. Left narrow band, right third octave bands

A possible source of error is in the measurement of force. This was independently checked by striking the attachment lug with a force hammer, i.e. with a known force. The transfer function departed from unity above about 600Hz, but the error was less than 3dB over most of the frequency range so would not have accounted for the differences observed.

Further discussion of the results is given in section 4.

3 MEASUREMENT USING AN INVERSE METHOD

The force transducer method described in the previous section is the most obvious technique to determine the blocked force of a laden motor. There are, however, problems with the technique. In particular it is difficult to insert force transducers between the motor and the block without compromising the stiffness of the attachment points.

The technique described in this section uses accelerometers to measure the motion of the suspended motor block, then applies Newtonian mechanics to work back to the forces applied. The advantages of this technique are that no sensors are required between the motor and the block so there is no disturbance to the local structural dynamics of the interface, to which contact forces can be highly sensitive [7]. Furthermore, there is less risk of compromising the 'blocking' of the motor attachment lugs.

3.1 Calculation of motor block transfer function

The centre-of-mass, moments of inertia and radii of gyration of the motor test block were calculated by dividing the block into simple solids (cuboids, cylinders and triangular prisms), calculating the parameters of each, then using the perpendicular and parallel axis theorems to determine the parameters of the whole block (see figure 1).

The calculated parameters, and the assumption of mass-like behaviour were validated by applying a force to a point on the block using an impact hammer and comparing the measured force with the force calculated from three accelerometers positioned on one face of the block. The transfer accelerance was calculated between the excitation point and the accelerometer positions using geometry and Newtonian mechanics. A least-squares-fit was used to back-calculate the applied force from the accelerometer measurements and this was compared with the actual force measured by a force transducer in the impact hammer. Figure 6 shows the ratio of the calculated force to the measured force and the difference in phase between the measured acceleration and the applied force. Note that frequencies where the calculated force was in error could be identified by phase shifts between the applied force and accelerometer measurements.

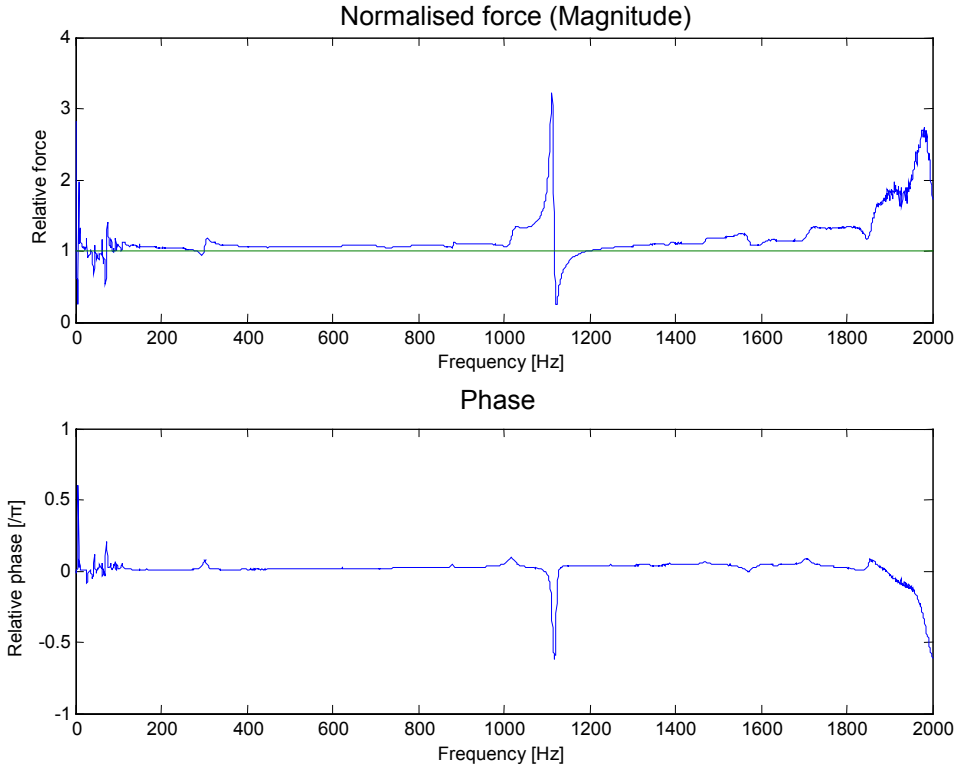

Figure 6: Ratio of calculated force to measured force (upper plot) and relative phase of measured acceleration to applied force (lower plot)

In order to extend the measurement, twelve accelerometer positions were selected, four each on the mutually orthogonal -X, +Y, and +Z faces of the block (see right hand side of figure 1). As the block was assumed to be rigid, the measured accelerations were not independent, and the maximum rank of the equations of motion was six, corresponding to the six degrees of freedom of the block. This led to a problem in determining the forces applied to the block by the motor, as the motor was attached at four lugs, implying twelve input forces (moments at individual attachment lugs were considered negligible). Some method was required to distribute the forces and moments between the four lugs.

As an interim step, the transfer accelerances were calculated between the accelerometers and a single point at the geometric centre of the four attachment lugs. This allowed the measured acceleration to be related to a hypothetical, equivalent force triplet and moment triplet applied at a single point on the block, such that $\mathbf{T} \cdot \mathbf{F} = \mathbf{A}$ where $\mathbf{F}$ is the column vector of three forces and three moments applied at the selected point, $\mathbf{A}$ is the column vector of twelve accelerations and $\mathbf{T}$ is the 12x6 element transfer matrix relating $\mathbf{F}$ and $\mathbf{A}$ (see equation 9).

$$\begin{bmatrix} t_{a1\,fx} & t_{a1\,fy} & t_{a1\,fz} & t_{a1mxx} & t_{a1myy} & t_{a1mzz} \\ t_{a2\,fx} & \cdot & \cdot & \cdot & \cdot & \cdot \\ \cdot & \cdot & \cdot & \cdot & \cdot & \cdot \\ \cdot & \cdot & \cdot & \cdot & \cdot & \cdot \\ \cdot & \cdot & \cdot & \cdot & \cdot & \cdot \\ \cdot & \cdot & \cdot & \cdot & \cdot & \cdot \\ \cdot & \cdot & \cdot & \cdot & \cdot & \cdot \\ \cdot & \cdot & \cdot & \cdot & \cdot & \cdot \\ \cdot & \cdot & \cdot & \cdot & \cdot & \cdot \\ \cdot & \cdot & \cdot & \cdot & \cdot & \cdot \\ \cdot & \cdot & \cdot & \cdot & \cdot & \cdot \\ t_{a12\,fx} & \cdot & \cdot & \cdot & \cdot & t_{a12mzz} \end{bmatrix} \cdot \begin{bmatrix} f_x \\ f_y \\ f_z \\ m_{xx} \\ m_{yy} \\ m_{zz} \end{bmatrix} = \begin{bmatrix} a_1 \\ a_2 \\ \cdot \\ \cdot \\ \cdot \\ \cdot \\ \cdot \\ \cdot \\ \cdot \\ \cdot \\ \cdot \\ a_{12} \end{bmatrix}$$

3.2 Measurement of block acceleration and calculation of equivalent forces

The motor was attached to the motor block and the whole assembly was suspended resiliently using steel cables and a hoist. Measurements of the acceleration at the twelve accelerometer positions were taken for nominal motor speeds of 2995, 7436, 12688, 14352 and 16224 rpm.

Measurements were taken using a four-channel FFT frequency analyser. The accelerometer connected to channel 1 was left in the same place throughout the measurement to give a common phase reference whilst the remaining three accelerometers were moved and measurements repeated to obtain the accelerations for each of the 12 positions.

The autospectrum and phase angle with respect to channel 1 was used to calculate the complex acceleration for each accelerometer as a function of frequency (bandwidth 0 to 2kHz), which was assembled to form the $\mathbf{A}$ vector for each frequency value.

A least-squares-fit was performed for each frequency to determine the value of equivalent force and moment vector, $\mathbf{F}$, from $\mathbf{A}$ and $\mathbf{T}$.

3.3 Distribution of equivalent force and moment vector between motor attachment points

In order to obtain the blocked forces at the attachment points between the motor and the block it was necessary to make a number of assumptions so that the equivalent force and moment vector could be distributed between the four attachment lugs. The assumptions made were;

1. That the moments applied to an individual attachment lug were likely to be small, compared with the ‘overall’ moments caused by force couples across the length or width of the motor, and could be neglected.
2. That below some frequency limit, f_L, the motor would act as a rigid mass, with blocked forces in-phase with one another at the motor attachment lugs.

3. That above f_L, the motor would no longer act as a rigid mass and the phases of the forces on the attachment lugs could be considered to be random with respect to one another.

In order to apply assumptions 2 and 3 it was necessary to determine the frequency, f_L, defining the limiting frequency of rigid mass behaviour of the motor. This was taken as the frequency of the anti-resonance between the mass and stiffness controlled regions of the motor point mobility. The point mobility was measured at the attachment lugs of the motor using an impact hammer and accelerometers, and sample plots are shown in figure 2.

3.3.1 Mass controlled region

For the frequencies below f_L the forces in vector $\mathbf{F}$ were simply divided equally between the four lugs, and the moments were decomposed into equal and opposite force couples which were also divided equally between the four lugs. A transfer function, $\mathbf{T2}$, was generated such that $\mathbf{F} = \mathbf{T2} \times \mathbf{G}$, where $\mathbf{G}$ is the vector of 12 blocked forces at the motor attachment lugs.

$$\begin{bmatrix} f_x \\ f_y \\ f_z \\ m_{xx}/a \\ m_{yy}/b \\ m_{zz}/a \end{bmatrix} = \begin{bmatrix} 1 & 1 & 1 & 1 & 0 & 0 & 0 & 0 & 0 & 0 & 0 & 0 \\ 0 & 0 & 0 & 0 & 1 & 1 & 1 & 1 & 0 & 0 & 0 & 0 \\ 0 & 0 & 0 & 0 & 0 & 0 & 0 & 0 & 1 & 1 & 1 & 1 \\ 0 & 0 & 0 & 0 & 0 & 0 & 0 & 0 & 1 & -1 & -1 & 1 \\ 0 & 0 & 0 & 0 & 0 & 0 & 0 & 0 & -1 & -1 & 1 & 1 \\ -1 & 1 & 1 & -1 & a/b & a/b & -a/b & -a/b & 0 & 0 & 0 & 0 \end{bmatrix} \cdot \begin{bmatrix} g_{1x} \\ g_{2x} \\ g_{3x} \\ g_{4x} \\ g_{1y} \\ g_{2y} \\ g_{3y} \\ g_{4y} \\ g_{1z} \\ g_{2z} \\ g_{3z} \\ g_{4z} \end{bmatrix}$$

Equation 10 shows the form of the relationship between $\mathbf{F}$ and $\mathbf{G}$ and the value of $\mathbf{T2}$, where a is the width of the block between lugs in the y direction, and b is the height of the block between lugs in the x direction.

Note that equation 10 is under-determined, and in order to estimate a solution we apply the assumption (which is implicit in the assumption that the motor acts as a rigid mass) that the most likely solution for $\mathbf{G}$ is the least energy solution resulting in the lowest norm of $\mathbf{G}$. This solution can be conveniently calculated by using the Moore-Penrose pseudoinverse of the matrix $\mathbf{T2}$, using the equation,

$$\mathbf{G} = \mathbf{T2}^{+} \times \mathbf{F}$$

where $\mathbf{T2}^{+}$ is the Moore-Penrose pseudoinverse of $\mathbf{T2}$.

3.3.2 Stiffness controlled region

For the frequencies above f_L we assumed that the forces in the individual attachment lugs were at random phases with respect to one another. As the forces in vector $\mathbf{F}$ represent the sums of these individual forces over the four lugs we can use the relationship,

$$|f|^2 = g_1^2 + g_2^2 + g_3^2 + g_4^2$$

where f is an element of $\mathbf{F}$ (the overall force), and g is an element of $\mathbf{G}$ (i.e. the force on an individual lug). Hence, using a similar technique as that of section 3.3.1 we define a transfer function, $\mathbf{T3}$, which relates the vector of $|f|^2$ values to the vector of $|g|^2$ values,

$$\begin{bmatrix} |f_x|^2 \\ |f_y|^2 \\ |f_z|^2 \\ |m_{xx}/a|^2 \\ |m_{yy}/b|^2 \\ |m_{zz}/a|^2 \end{bmatrix} = \begin{bmatrix} 1 & 1 & 1 & 1 & 0 & 0 & 0 & 0 & 0 & 0 & 0 & 0 \\ 0 & 0 & 0 & 0 & 1 & 1 & 1 & 1 & 0 & 0 & 0 & 0 \\ 0 & 0 & 0 & 0 & 0 & 0 & 0 & 0 & 1 & 1 & 1 & 1 \\ 0 & 0 & 0 & 0 & 0 & 0 & 0 & 0 & 1 & 1 & 1 & 1 \\ 0 & 0 & 0 & 0 & 0 & 0 & 0 & 0 & 1 & 1 & 1 & 1 \\ 1 & 1 & 1 & 1 & a^2/b^2 & a^2/b^2 & a^2/b^2 & a^2/b^2 & 0 & 0 & 0 & 0 \end{bmatrix} \cdot \begin{bmatrix} |g_{1x}|^2 \\ |g_{2x}|^2 \\ |g_{3x}|^2 \\ |g_{4x}|^2 \\ |g_{1y}|^2 \\ |g_{2y}|^2 \\ |g_{3y}|^2 \\ |g_{4y}|^2 \\ |g_{1z}|^2 \\ |g_{2z}|^2 \\ |g_{3z}|^2 \\ |g_{4z}|^2 \end{bmatrix}$$

Again, the equation is solved for values of $|g|^2$ using the Moore-Penrose pseudoinverse of **T3**, and square-roots are taken of the solution vector to obtain **G** (note that phase relationships between applied force and accelerations were lost for the stiffness controlled region).

The **G** vectors for frequencies below f_L determined in section 3.3.1, and those for frequencies above f_L determined above, were then combined to obtain values of blocked-force for the whole frequency range.

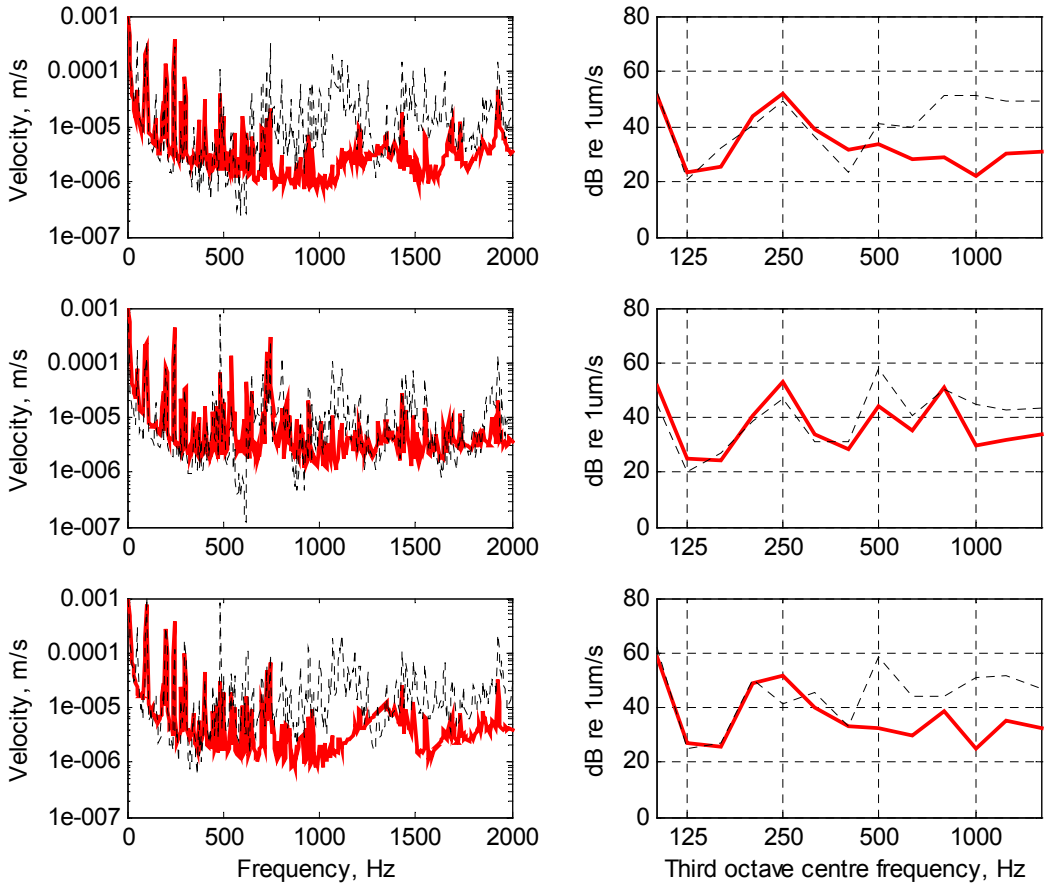

Figure 7: Results for inverse technique for lug 4 at 14352 rpm: ¯ measured free velocity, --- calculated. Directions, from top to bottom; x, y, z. Left narrow band, right third octave bands

3.4 Validation

In order to validate the blocked force measurement made above, it was compared with the 'free velocity' of the motor attachment lugs in the same way as described in section 2. Measurements were carried for motor A2 only at four speeds.

Example comparisons between the free velocities measured for the freely suspended motor and those calculated from the blocked force are shown in figures 7-8. Figure 7 shows comparisons between the x, y and z direction free velocities for a particular lug at a single speed. Similar plots were obtained for other mounting lugs and other speeds. Figure 8 shows comparisons between the energy averaged (overall) free velocity in the *y* direction.

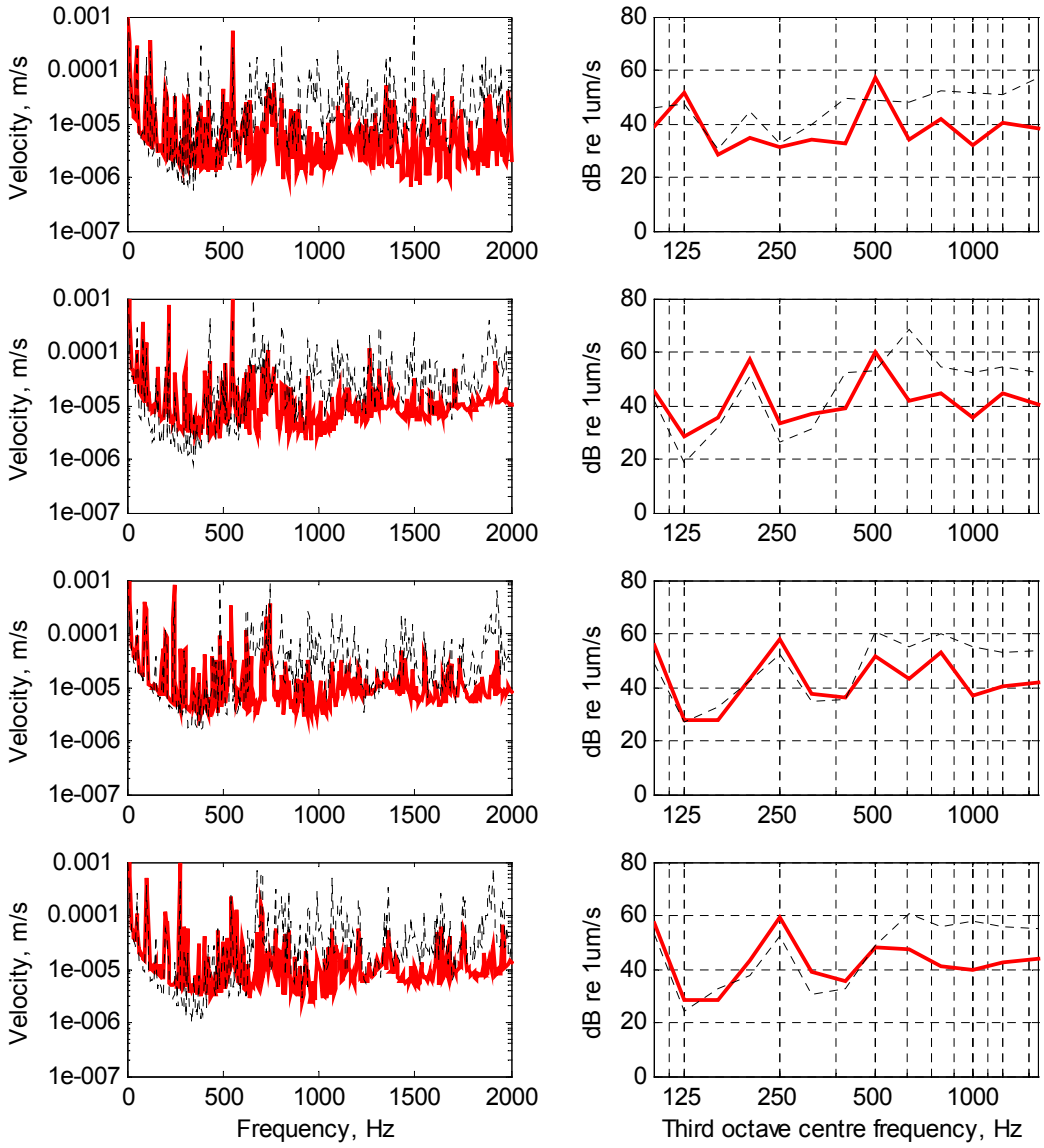

Figure 8: Motor A2 results for inverse technique energy averaged over lugs in y direction: — measured free velocity, --- calculated at running speeds of, from top to bottom 7436, 12688, 14352 and 16224 rpm. Left narrow band, right third octave bands

The plots for the individual lugs show good agreement below 600 Hz. Above this frequency the prediction is generally high and there are differences in terms of peak positions compared with the measured values. Plots of the overall y direction velocity show similar behaviour with reasonably accurate predictions below 400Hz for the highest three speeds, and with rather less accurate prediction at the lowest running speed. Similar trends were observed in the z direction results (not shown). From 400 Hz the broadband calculated values are consistently higher than those measured directly, with the exception of the 500 Hz band measured in the *y* direction, and at the lowest motor speed in the *z* direction.

4 DISCUSSION OF RESULTS

There are similarities in both sets of results in that general agreement is good at low frequencies. Results for motor A2 (not shown for force transducer method due to lack of space) were similar for both methods in that the blocked force results were systematically higher than the directly measured free velocity in the higher part of the range. This could suggest that the errors are due to the validation procedure or in differences in the operation of the motor between the free and blocked conditions.

A possible source of error is in the mobility matrix used for the transformation, which was obtained on a different, although nominally identical motor housing. Such an error would affect both sets of results in a similar way. Referring to the plot of the mobility in figure 2, the motor broadly speaking behaves as a rigid mass up to about 400Hz, and a local spring up to about 1200Hz, above which it exhibits resonant behaviour. All results agree reasonably well in the frequency range where the motor is mass like, and less well when the motor is resonant. It is most likely, if there are differences in mobility from one motor housing to another, that this would show up in the resonant region. This will be investigated further at a later date.

A related source of error that would affect both sets of results is that in applying the mobility model (equation 6) it is assumed that the motor feet make point contact, and furthermore that they are ‘pinned’, i.e. they are not constrained by moments. Petersson [5] has shown that in certain circumstances neglecting moments can cause errors, and this was also found to be the case for a real fan in reference [2]. Such errors tend to be greater at higher frequencies [6] which is consistent with the findings here. If these assumptions are not met then an error will be incurred in transforming the blocked forces to free velocities i.e. the validation will be in error, not necessarily the blocked forces themselves. It is the author’s experience that to include moments often causes greater errors because of the difficulty of measuring reliable moment mobilities. Therefore, this source of error cannot easily be removed, except perhaps by using a hybrid, measured-calculated mobility matrix as described in [2].

It is also possible that the vibration generating mechanisms in a free and blocked motor are different. This is conceivable, for example if the act of bolting the motor to the block caused distortion of the casing which affected rotor-stator concentricity, and one can theorise other such mechanisms. One observation of relevance here is that the spectral shape of the error is broadly the same for all operating speeds and both sets of results. This suggests that it is due to passive, structural dynamic effects rather than the actual source mechanisms which would be expected to ‘follow’ the harmonic series as the speed varied. A possible way to evaluate this effect would be to obtain the characteristic power [8] with the contact points in various degrees of constraint between free and blocked. The characteristic power is based on the product of the free velocity and blocked force vectors, and should be invariant to the mounting condition unless the generating mechanisms vary. Variation in the characteristic power would then indicate that source mechanisms are varying.

One other observation worth mentioning is that the agreement was generally better for the higher motor running speeds. This trend was observed also in other tests with the motor, including tests and predictions of airborne sound output. A possible explanation is that the noise generating mechanisms are more stable and repeatable at high speed.

5 CONCLUDING REMARKS

In order to construct virtual acoustic prototypes of machines it is necessary to characterise the active components' ability to excite the rest of the structure. The free velocity is often used as an 'activity' parameter, but it cannot be measured directly for electric motors under load. Hence this paper investigates the use of an alternative, the blocked force.

Two methods of blocked force measurement have been investigated: direct measurement with force transducers inserted between the motor and a mounting block, and indirect, using Newtonian mechanics to infer forces from the motion of the block. An independent validation has been achieved using the measured free velocity.

Reasonable agreement has been obtained between the directly measured free velocity and that obtained from the blocked forces in the lower part of the frequency range (up to about 500Hz). In this range the motor is compact and behaves like a rigid mass. At higher frequencies both methods show significant errors. We can conclude that either method should give reasonable results for a compact source, but the force transducer results are the better of the two.

The discrepancies show similar trends for both types of measurement and for all speeds. This suggests that the lack of agreement at higher frequency could be due to differences in motor operation in 'free' and 'blocked' conditions. Alternatively, it may be that the validation procedure is in error.

6 REFERENCES

1. BS ISO 9611:1996. Acoustics. Characterization of sources of structure-borne sound with respect to sound radiation from connected structures. Measurement of velocity at the contact points of machinery when resiliently mounted.
2. A T MOORHOUSE, Use of a hybrid measured-calculated mobility matrix for simplified calculation of structure-borne sound from an electric motor, Proc. 10th ICSV, Stockholm, 2003
3. MONDOT, J M MOORHOUSE A T, The characterisation of structure-borne sound sources, Proc Inter-noise 96, Book 3, 1439-1446, Liverpool 1996.
4. B A T PETERSSON and A T MOORHOUSE, Interface mobilities for source characterisation; matched conditions. Proc. 7th ICA, Rome 2001.
5. PETERSSON BAT 1993, JSV, 160(1), p 43-66. Structural acoustic power transmission by point moment and force excitation, part I: beam-like and frame-like structures.
6. PETERSSON BAT, GIBBS BM Use of the source descriptor concept in studies of multipoint and multidirectional vibrational sources. J SOUND VIB 168 (1): 157-176 1993
7. A T MOORHOUSE and J X SU, Statistical mobility for multiple point excited structures, Proc. 8th ICSV, Hong Kong, 2001
8. A T MOORHOUSE, 'On the Characteristic Power of structure-borne sound sources', Journal of Sound and Vibration , 248 (3): 441-459, 2001